Title
Mechanism of tumor destruction following photodynamic therapy with hematoporphyrin derivative, chlorin, and phthalocyanine.

Journal
Journal of the National Cancer Institute, 80(20)

ISSN
0027-8874

Authors
Nelson, JS
Liaw, LH
Orenstein, A
et al.

Publication Date
1988-12-01

DOI
10.1093/jnci/80.20.1599

ARTICLES

Mechanism of Tumor Destruction Following Photodynamic Therapy With Hematoporphyrin Derivative, Chlorin, and Phthalocyanine

J. Stuart Nelson, Lih-Huei Liaw, Arie Orenstein, W. Gregory Roberts, Michael W. Berns*

The effect of photodynamic therapy on the tumor microvasculature in the first few hours after treatment was studied at the light and electron microscopy levels. BALB/c mice with EMT-6 tumor received ip injections of hematoporphyrin derivative, chlorin, or phthalocyanine, and 24 hours later, the tumors were treated with light at 100 J/cm^2 at the appropriate therapeutic wavelength for each photosensitizer. Animals were killed and their tumors removed at time 0, 30 minutes, 1 hour, and 2, 4, 6, 8, 12, 16, and 24 hours after treatment. The results indicate that for all three sensitizers the effects of photodynamic therapy leading to rapid necrosis of tumor tissue are not the result of direct tumor cell kill but are secondary to destruction of the tumor microvasculature. The first observable signs of destruction occur in the subendothelial zone of the tumor capillary wall. This zone, composed of dense collagen fibers and other connective tissue elements, is destroyed in the first few hours after phototherapy. However, the ultrastructural changes seen in this zone are different for the hematoporphyrin derivative, compared with chlorin and phthalocyanine. Binding of photosensitizers to the elements in this zone as well as altered permeability and transport through the endothelial cell layer because of the increased intraluminal pressure may be key features of tumor destruction. [J Natl Cancer Inst 1988;80:1599-1605]

During the past several years, many photosensitizing porphyrins have been shown to be retained selectively in rapidly growing, solid tumors in humans and other mammals (*1*). The action of these photosensitizers is to absorb photons of the appropriate wavelength sufficient to elevate the sensitizer to an excited state. The excited photosensitizer subsequently reacts with a molecular substrate, such as oxygen, to produce singlet oxygen, which causes irreversible oxidation of some essential cellular component (*2*). Uncertainty arises as to the exact cellular targets of these excited intermediates, although damage to the cell membrane (*3*), mitochondria (*4*), lysosomes (*5*), and the nuclear material (*6*) have been reported.

Shortly after treatment, the tumor becomes necrotic (usually within 24 hr), and when effectively treated, the tumor becomes a nonpalpable scab that is usually sloughed within a few days. A wide variety of tumors with varying histologic types have been treated with photodynamic therapy (PDT) including cancers of the skin (*7*), female genital tract (*8*), esophagus (*9*), lung (*10*), bladder (*11*), eye (*12*), and breast (*13*), and head and neck squamous cell carcinomas (*14*). Treatment parameters have been refined such that therapy can be undertaken with a reasonable expectation of good results in both animal and human trials. Although PDT can be used to eradicate relatively large tumors, it appears especially advantageous to the patient with superficial early disease or early recurrence. In addition, previous surgery, radiation therapy, or chemotherapy does not preclude the use of PDT, and many of the clinical studies reported to date have been on patients who have not benefited from some or all other forms of therapy.

Received July 13, 1988; revised October 14, 1988; accepted October 18, 1988.

Supported in part by Public Health Service grants RR-01192 from the Division of Research Resources, and CA-32248 from the National Cancer Institute, National Institutes of Health, Department of Health and Human Services; and grant SDI084-88-C-0025 from the Department of Defense.

Department of Surgery, and the Beckman Laser Institute and Medical Clinic, University of California, Irvine, Irvine, CA.

We thank Dr. Kevin Smith, University of California at Davis, for providing the mono-L-aspartyl chlorin e_6; Jeffrey Andrews and Glen Profeta for their technical assistance in operating the lasers; and Ms. Elaine Kato for preparation of the manuscript.

**Correspondence to:* J. Stuart Nelson, M.D., Beckman Laser Institute and Medical Clinic, 1002 Health Sciences Road East, Irvine, CA 92715.

Despite these positive attributes, some of the fundamental mechanisms involved in this unique application of photochemotherapy remain incompletely understood. For example, it is still not known whether tumor destruction is a result of actual PDT phototoxic effects on the proliferating tumor cell or, as has been recently suggested, the result of damage produced to some other tumor elements, such as the microvasculature (*15*). Apparent internal hemorrhage and red cell extravasation are common findings after PDT, not only in most experimental animal tumors but in tumors in patients as well. With this in mind, our objective in this study was to examine the ultrastructural effects of several photosensitizers on the tumor microvasculature during the first few hours after phototherapy. We hope that this type of study will help elucidate the complex role of the tumor vasculature in PDT as well as provide a basic understanding of the mechanism of phototoxicity of potential new photosensitizers.

Materials and Methods

Animal and Tumor System

The EMT-6 experimental mammary tumor arising in the flanks of BALB/c mice was used. All mice were 6–8 weeks old and weighed between 30 and 35 g at the time of treatment. When the tumors attained a size of 1–2 cm in diameter, they were excised and minced with fine scissors in phosphate-buffered saline (PBS). This resulting suspension of tumor cells was filtered through sterile gauze, washed twice in PBS, and then resuspended in RPMI media (GIBCO, Grand Island, NY) at a concentration of 5×10^5 viable cells/mL. Viability of the cells was assessed by their ability to resist lysis and exclude Trypan Blue dye (GIBCO). We initiated the tumors by injecting 0.1 mL of fresh tumor inoculum into the right flank of mice. The mouse tumors were generally palpable at 5 days and reached a size of 5–7 mm by 10–14 days at which time we started the treatment. At this size, the small tumors were homogeneously white, with spontaneous tumor necrosis minimal or absent.

Photosensitizers

For all photosensitizers, a drug dose was chosen that would ensure complete tumor kill in all animals tested.

Photofrin II [(DHE); Photomedica, Inc., Raritan, NJ] was obtained as an aqueous solution at a concentration of 2.5 mg/mL and stored in the dark at −70 °C until used. For in vivo experiments, DHE was diluted 1:4 with 0.9% NaCl solution and injected ip in doses equal to 10 mg/kg body weight (*16*).

Mono-L-aspartyl chlorin e_6 (MACE) was received as a dark green powder, reconstituted in Dulbecco's PBS to a final concentration of 2.5 mg/mL, and stored in the dark at −70 °C until used (*17*). Prior to injection, MACE was diluted 1:4 with 0.9% saline solution and injected ip in doses equal to 10 mg/kg body weight (*18*).

Chloroaluminum sulfonated phthalocyanine [(CASPc); Ciba-Geigy Corp., Basel, Switzerland] was provided as a 300-mg/mL sample in water. It was diluted in Dulbecco's PBS to a final concentration of 2.5 mg/mL and stored in the dark at −70 °C until used. Prior to injection, CASPc was diluted 1:4 with 0.9% saline solution and then given ip in doses equal to 1 mg/kg body weight.

Experimental Procedure

When the tumors reached the appropriate size of 5–7 mm, the animals were shaved in the tumor area and given ip injections of the photosensitizer; the remainder of the experiment was done in the dark, including housing of the animals. Control tumor-bearing animals received light without photosensitizer and photosensitizer without light. Twenty-four hours after the injections, the animals were treated with a laser light delivery system. The mice were anesthetized with ketamine hydrochloride (Parke-Davis, Morris Plains, NJ) and covered with a metal shield with a circular hole exposing the tumor. Animals were killed with Halothane (Halocarbon Laboratories, Inc., Hackensack, NJ) at time 0, 30 minutes, 1 hour, and 2, 4, 6, 8, 12, 16, and 24 hours after exposure to the laser light. Tissue was excised immediately and placed in Karnovsky's fixative (2% paraformaldehyde; 3% glutaraldehyde), refrigerated overnight at 4 °C, and subsequently transferred to 0.1 *M* cacodylate buffer until electron microscopy embedding was performed. The tissue was postfixed in 1% osmium tetroxide in 0.1 *M* cacodylate buffer for 1 hour at room temperature (18 °C – 20 °C). Tissue was then rinsed with double distilled water and stained en bloc for 2 hours in Kellenberger's uranylacetate. Dehydration was done with progressive ethanol–water in 10-minute steps (30%, 50%, 70%, 90%, 100%, 100%) and progressive ethanol–propyleneoxide also in 10-minute steps. Infiltration was started with propyleneoxide-Epon 812 substitute [Poly/Bed 812 Embedding Media (Polysciences Inc., Warrington, PA)] in steps of 30 minutes each (30%, 50%), overnight (70%), and 60 minutes (100%). The mold was embedded, placed at 37 °C overnight, and then at 60 °C in a vacuum oven for 48 hours. The blocks were trimmed, sectioned (500 nm), and stained for light microscopy with Richardson's stain. The thin-sectioned (60 nm) blocks were subsequently examined with a Jeol 100C electron microscope at 80 kV.

Laser Light Delivery System

Laser irradiations were performed with a 770DL argon pumped dye laser system (Cooper Lasersonics, Santa Clara, CA) and DCM Premixed Laser Dye (Cooper Lasersonics) with a tuning range of 610–690 nm. The dye laser was tuned to emit radiation at 630 nm for DHE, 664 nm for MACE, and 675 nm for CASPc. We verified the wavelength to ± 1 nm by using a #5/354 UV monochromator (Jobin Yvon, Longjuneau, France). The radiation was then transferred with a Model 316 fiber optic coupler into a 400-μm fused, silica fiber optic (Spectra-Physics, Mountain View, CA). We terminated the output end of the fiber with a microlens that focused the laser radiation into a circular field of uniform light intensity. The laser irradiation that emanated from the fiber was monitored with a Coherent Model 210 power meter before, during, and after treatment.

Mice were then placed underneath an aperture that controlled the area of light illumination on the tumor site; the

area of illumination was 1 cm^2. Total laser energy density, 100 J/cm^2, had a power density of 100 mW/cm^2.

Results

Light Microscopy

Control (either light or drug alone) slides showed the usual tumor architecture with multiple mitotic figures and easily discernible vessels. At 30 minutes after PDT, no significant structural changes were noted from the control. At 1 hour afterward, the first structural change observed with all photosensitizers tested was the increased diameter of the tumor capillary lumen compared with controls. Of particular interest was the large diameter (swelling) of the erythrocytes in the swollen vessels. This conclusion was based on the histopathologic examination of all sections and tumors and was not attributable to the way a particular section was cut. At 2 hours, the capillaries were further engorged, and, over time, the capillary wall broke down with extravasation of erythrocytes into the surrounding perivascular tumor stroma with the tumor ultimately becoming completely hemorrhagic. This observation was made for all photosensitizers tested (fig. 1).

Electron Microscopy

Control ultrathin sections showed normal tumor microvasculature with the subendothelial zone densely packed with large amounts of collagen, elastic and reticular fibers, and background connective tissue elements, especially proteoglycans (fig. 2). Generally, the lumen of each tumor capillary was surrounded by three to four endothelial cells in junctional contact with each other. The tumor cells in the surrounding perivascular tumor stroma appeared structurally intact with large numbers of mitochondria, endoplasmic reticulum, and ribosomes. At 30 minutes after completion of PDT, there were no significant structural changes from controls noted in the microvasculature or the tumor cells.

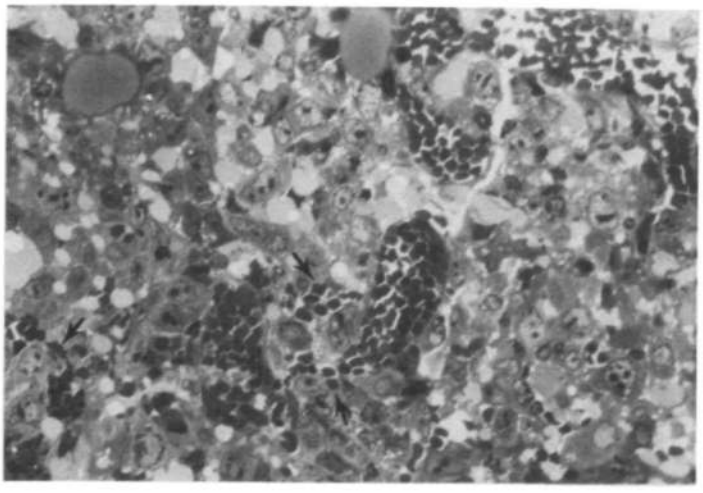

Figure 1. Photomicrograph of EMT-6 tumor removed 4 hr after treatment with photosensitizer and light at total dose of 100 J/cm^2. Note evidence of extravasation of erythrocytes into the surrounding perivascular tumor stroma (arrows). Originally: ×700.

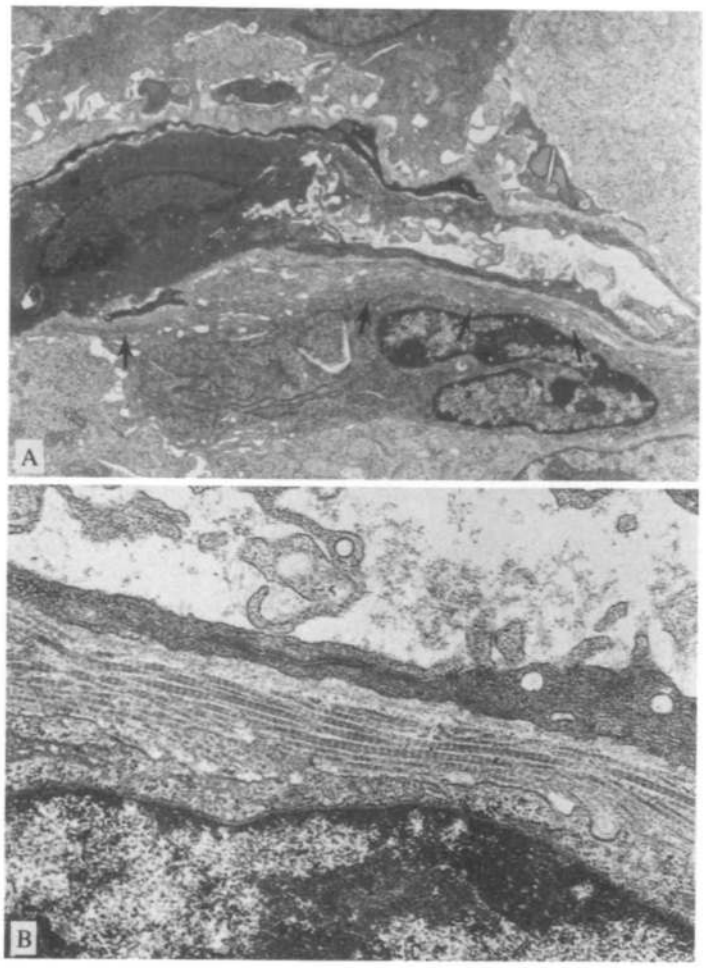

Figure 2. Photomicrographs of control tumor (no photosensitizer, no light) showing normal tumor microvasculature (A) with the subendothelial zone (arrows) densely packed with large amounts of collagen, elastic and reticular fibers, and background connective tissue elements (B). Originally: A, ×6,000; B, ×28,100.

One hour after completion of PDT with MACE (fig. 3) and CASPc (fig. 4), injury to the subendothelial zone of the capillary wall was characterized by considerable edema and fragmentation of the collagen and fiber elements. The endothelial cells lining the capillary wall appeared elongated and flat compared with our controls with smooth luminal and abluminal surfaces but were otherwise structurally normal. The nuclei had the typical chromatin condensation along the nuclear envelope, normal rough endoplasmic reticulum, and membrane-bound lysosomes were evident in the cytoplasm. Erythrocyte swelling described above was also seen. By 2 hours post PDT, the background substance was essentially absent, and only a few fragmented collagen fibers remained in the subendothelial zone in the MACE- and CASPc-treated tumors (fig. 5).

One hour after completion of PDT with DHE, some of the ultrastructural changes in the subendothelial zone were strikingly different from those observed in tumors treated with MACE or CASPc. At 1 hour post PDT, the subendothelial zone was more darkly stained, and individual collagen fibers were no longer clearly distinguished (fig. 6). However,

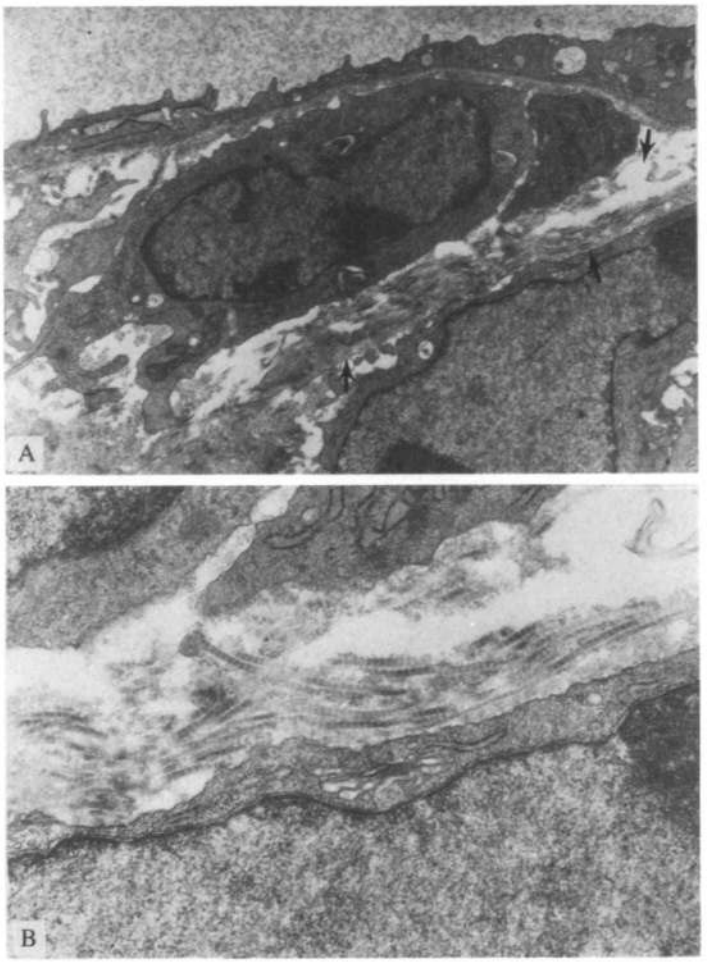

Figure 3. Photomicrographs of tumor removed 1 hr after treatment with MACE and light. Note in the subendothelial zone (arrows) the formation of considerable edema (A) and fragmentation of the collagen and other fiber elements (B). Originally: A, ×9,000; B, ×26,600.

as with the MACE- and CASPc-treated tumors, the vessels were swollen, erythrocytes were enlarged, and considerable edema was observed in the subendothelial zone. At 2 hours after treatment, the background substance in the subendothelial zone was essentially destroyed and replaced by edema, but numerous clusters still contained large amounts of fibers and fibrin that appeared to have coalesced. Furthermore, delineation of the characteristic periodicity and banding pattern of collagen fibers was difficult (fig. 7).

Beyond 2 hours posttreatment, the subendothelial zone was completely disrupted, although there was still some evidence of fibrin. Erythrocytes and plasma proteins were extravasated into the subendothelial zone and subsequently into the region of the tumor cells immediately adjacent to the microvasculature with the three photosensitizers tested (fig. 8). Tumor cells closer to the hemorrhage showed more signs of cell membrane damage and lysis. However, tumor cells distant from the microvasculature in the center of the tumor appeared to have their cell membranes structurally intact even 4 hours after PDT. In those cells, dispersion of the heterochromatin around the nuclear envelope was apparent as well as some increase in the number of cytoplasmic vacuoles (fig. 9). Beyond 4 hours, the amount of hemorrhage increased with the entire tumor ultimately becoming a sea of erythrocytes and amorphous granular debris.

Discussion

Although most investigators to date have focused their research on understanding the biochemistry, biophysics, and molecular biology of PDT on cancer cells in vitro, less attention has been paid to the in vivo tumor environment where the photochemistry leading to tumor necrosis occurs. However, it is apparent that the exact mechanism of PDT phototoxicity in vivo will have to be explained by the anatomy, physiology, and biochemistry of the whole tumor rather than on the basis of some special characteristic of malignant tumor cells. Once a molecule used for cancer detection or treatment is injected into the bloodstream, it must first be distributed throughout the vascular space. Because no molecule can reach tumor cells from the blood without passing through the microvascular wall, it seems reasonable that investigators should attempt to learn more about the role that this compartment plays in PDT.

Some progress has been made recently in our understanding how the microvasculature may be involved in the events leading to tumor necrosis. Several investigators (*19,20*) have

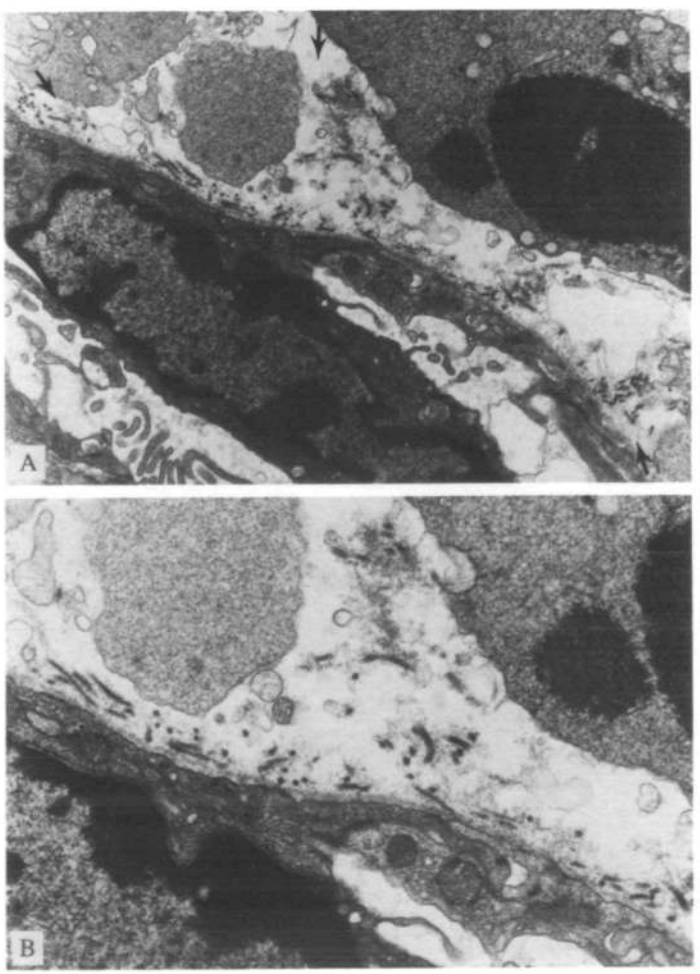

Figure 4. Photomicrographs of tumor removed 1 hr after treatment with CASPc and light. Note in the subendothelial zone (arrows) the formation of considerable edema (A) and fragmentation of the collagen and other fibers (B). Originally: A, ×15,000; B, ×26,600.

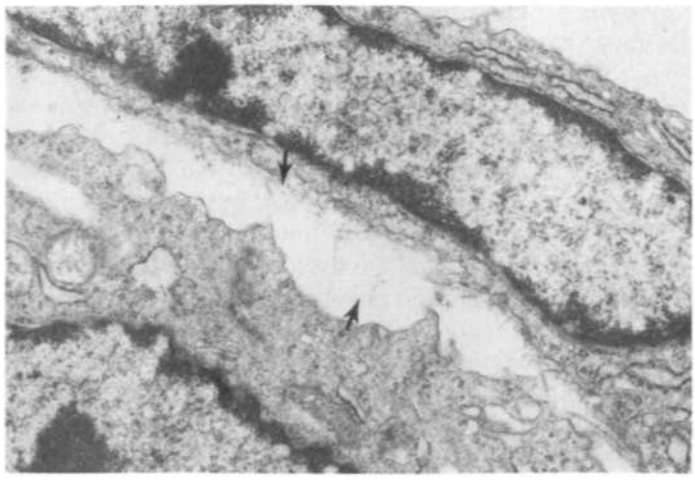

Figure 5. Photomicrograph of tumor removed 2 hr after treatment with MACE and light. Background substance was essentially absent and only a few fragmented collagen fibers remained in the subendothelial zone (arrows). Originally: ×24,400.

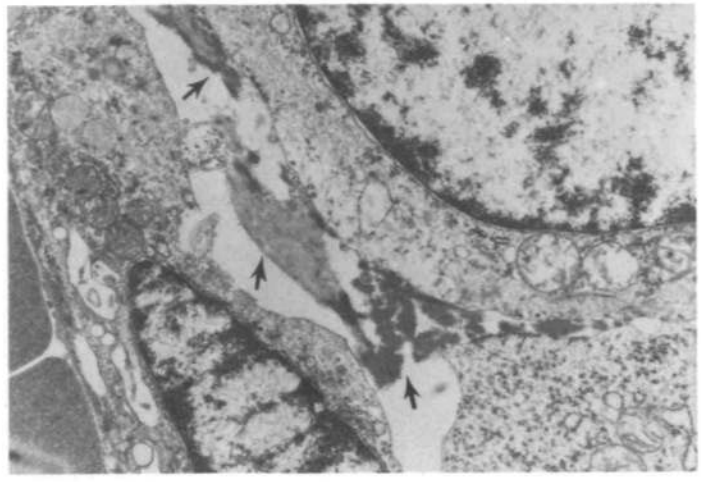

Figure 7. Photomicrograph of tumor removed 2 hr after treatment with DHE and light. Background substance in the subendothelial zone was essentially destroyed and replaced by edema, but note the presence of numerous clusters of fibers and fibrin that appeared to have coalesced (arrows). Furthermore, delineation of characteristic periodicity and banding pattern of collagen fibers was difficult. Originally: ×15,000.

shown that within a few minutes of light exposure, the significant decrease in the rate of blood flow through tumors is followed shortly thereafter by complete cessation. In addition, researchers in another study, using tumor cell clonigenicity following PDT to assess in vitro colony formation, found that it was unaffected by PDT if the tumor tissue was excised and explanted immediately. If, however, tumor cells were left in situ following PDT for varying periods, tumor cell death occurred rapidly and progressively as assayed by clonigenicity (*21*). Taken together, all these experiments suggest that the vascular compartment represents an important target for PDT and that more detailed studies should be undertaken.

Our objective in this study was to determine the ultrastructural changes seen in the tumor microvasculature in vivo in the first few hours after PDT. Clearly, many physiologic parameters of blood vessels, such as blood flow, pH, oxygen tension, temperature, and serum content, will be important. However, our study demonstrates that the first observable signs of destruction occur in the subendothelial zone of the tumor capillary wall. Blood vessels contain endothelial cells that are surrounded by a basement membrane, which may be damaged or missing in tumors (*22*). Adjacent to this is a subendothelial or interstitial compartment bounded by the basement membrane on one side and by the membranes of tumor cells on the other. Similar to normal blood vessels, the subendothelial zone of tumor vessels is composed predominantly of a dense collagen, elastic, and reticular fiber network. Interspersed within this cross-linked structure are the macromolecular polysaccharide constituents (proteoglycans and hyaluronate) that form a gellike background substance (*23*). This zone, which maintains the structural in-

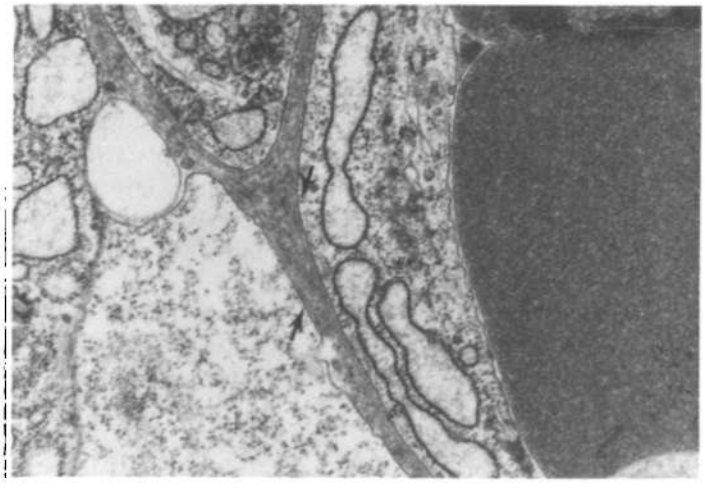

Figure 6. Photomicrograph of tumor removed 1 hr after treatment with DHE and light. Note the presence of large numbers of dense dark staining clumps of fibers in the subendothelial zone (arrows). Individual collagen fibers were no longer clearly distinguished. Originally: ×28,900.

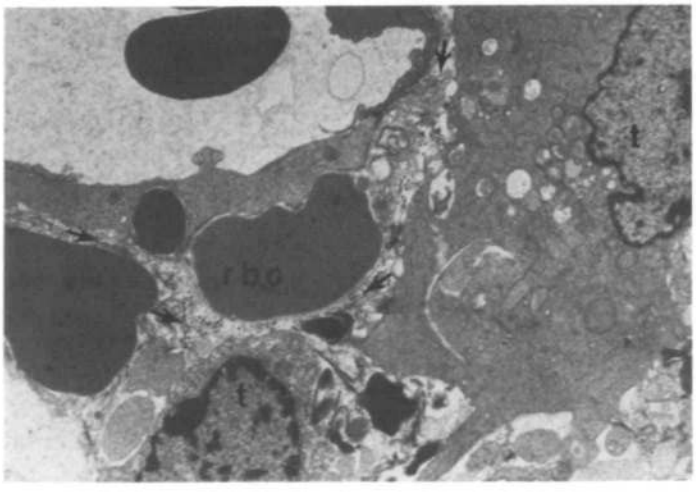

Figure 8. Photomicrograph of tumor removed 2 hr after treatment with CASPc and light. Subendothelial zone (arrows) was completely disrupted, although there was still some evidence of fibrin, with extravasation of red blood cells (rbc) into this area. Tumor cells (t) closer to this hemorrhage showed more signs of cell membrane damage. Originally: ×9,600.

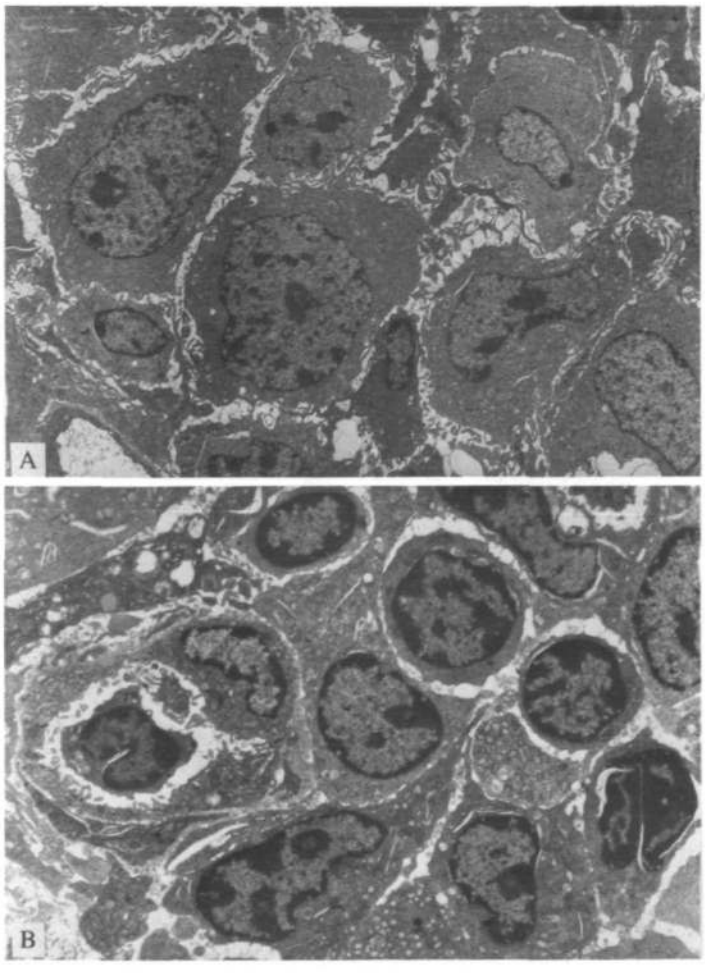

Figure 9. Photomicrographs of control tumor (A) and tumor removed 4 hr after treatment with MACE and light (B). Treated tumor cells distant from the microvasculature in the center of the tumor have their cell membranes structurally intact. Some dispersion of the hematochromatin can be seen around the nuclear envelope as well as some increase in the number of cytoplasmic vacuoles (B). Originally: A, ×3,600; B, ×6,000.

tegrity of the tumor capillary wall, was destroyed within the first 2 hours after phototherapy with all three photosensitizers tested. We did note many normal appearing endothelial cells in areas where there was significant damage to the fibers in the subendothelial zone. The normal ultrastructure of the endothelial cells was surprising because these cells were suspected of being primary target sites of the dye-sensitized photodynamic reaction. However, the fact that no structural alteration of the endothelial cells was observed does not mean that their membrane permeability or junctional contacts were unaffected. In fact, their unusually flattened and elongated appearance as soon as 1 hour after PDT (undoubtedly caused by swollen erythrocytes) could have resulted in membrane stretching and altered junctional contacts. This phase was followed shortly by edema in the subendothelial zone and, ultimately, diffuse hemorrhage into the surrounding perivascular stroma. Initially, tumor cells located away from the microvasculature appeared structurally intact after PDT. Over time, all tumor cells were ultimately destroyed as a consequence of hemorrhage, activation of intravascular component such as complement, or hypoxia secondary to vascular collapse.

Why is the subendothelial zone of the tumor microvasculature so important to successful PDT? Part of the answer may come from in vitro and in vivo studies that have shown that a stabilized polysaccharide network (proteoglycans and hyaluronate) enmeshed in collagen fibers offers considerable resistance to interstitial transport (*24,25*). Although the insoluble, collagen fibrous proteins impart structural integrity to a tissue, the polysaccharides are thought to govern the mass transfer characteristics of the tissue due to their high-charge density. The biologic and physicochemical properties of this zone combined may retard the movement of photosensitizing compounds from the vascular space into the tumor cells. That the tumor collagen is produced by the host and its synthesis is governed by the tumor cells are particularly noteworthy (*26*). If tumor growth depends on collagen production to the extent that it depends on neovascularization, this characteristic of tumors may be exploited in arresting such growth. Tumor collagen fibers also resemble the types of fibers seen in embryonic tissue and in wounds during healing. That these fibers, recently made in the neovascularization of tumors, would not be as highly cross-linked as those found in more mature tissues is to be expected. Furthermore, one study (*27*) has shown that newly formed collagen and perhaps elastin and fibrin as well have a substantially greater binding capacity for porphyrins than does mature collagen and may constitute potentially important binding sites for porphyrin localization and retention.

The reason for the different ultrastructural changes seen with DHE as opposed to MACE and CASPc is less clear, but some possible explanations are proposed. Due to the internal structure of collagen (a cylindrical molecule composed of three chains coiled in a ropelike fashion to form a triple helix), fibers will have space within them that is probably accessible to small molecules and ions. DHE is highly hydrophobic and tends to aggregate into large molecules of 200–300 components. MACE and CASPc are hydrophilic, smaller molecules that may be able, on the basis of size, to become intercalated inside the coiled collagen helix. Such action could lead to the breakdown and fragmentation of the collagen fibers from the inside as we saw in this experiment. DHE may be confined to the outside of the collagen fiber leading to the coalescence of large clumps of collagen fibers seen on examination with electron microscopy. Additionally, collagen contains three specific amino acids (glycine, hydroxylysine, and hydroxyproline) that may interact with the available carboxy groups on MACE and the sulfonated groups on CASPc. These biologic and physicochemical characteristics could explain the ultrastructural differences observed for the different photosensitizers. Further research in this area is needed.

In conclusion, the present study suggests that the effects of PDT leading to rapid tumor necrosis with DHE, MACE, and CASPc are not the result of direct tumor cell kill but are secondary to destruction of the collagen fibers and other connective tissue elements located in the subendothelial zone of the tumor capillary wall. Binding of photosensitizers to the elements in this zone as well as altered permeability and transport through the endothelial cell layer resulting from erythrocyte swelling and increased intraluminal pressure may

be key features of the dye-sensitized, photodynamic reaction leading to tumor destruction.

References

1. DOUGHERTY TJ. Photosensitizers: therapy and detection of malignant tumors. Photochem Photobiol 1987;45:879-889.
2. WEISHAUPT KR, GOMER CJ, DOUGHERTY TJ. Identification of singlet oxygen as the cytotoxic agent in photoinactivation of a murine tumor. Cancer Res 1976;36:2326-2329.
3. GROSSWEINER LI. Membrane photosensitization by hematoporphyrin and hematoporphyrin derivative. In: Doiron DR, Gomer CJ, eds. Porphyrin localization and treatment of tumors. New York: Liss, 1984:391-404.
4. BERNS MW, DAHLMAN A, JOHNSON F, et al. In vitro cellular effects of hematoporphyrin derivative. Cancer Res 1982;42:2325-2329.
5. TORINUKI L, MIORA T, SEIJI M. Lysosome destruction and lipoperoxide formation due to active oxygen generated from hematoporphyrin on UV radiation. Br J Dermatol 1980;102:17-27.
6. FOOTE CS. Photosensitized oxidation and singlet oxygen: consequences in biological systems. In: Pryor WA, ed. Free radicals in biology, vol II. New York: Academic Press, 1976:85-124.
7. DOUGHERTY TJ. Photoradiation therapy for cutaneous and subcutaneous malignancies. J Invest Dermatol 1981;77:122-124.
8. RETTENMAIER MA, BERMAN ML, DISAIA PJ, et al. Gynecologic uses of photoradiation therapy. In: Doiron DR, Gomer CJ, eds. Advances in experimental medicine and biology, vol 170. New York: Liss, 1984:767-775.
9. DOUGHERTY TJ. Photodynamic therapy (PDT) of malignant tumors. CRC Crit Rev Oncol Hematol 1984;2:83-116.
10. HAYATA Y, KATO H. Applications of laser phototherapy in the diagnosis and treatment of lung cancer. Jpn Ann Thoracic Surg 1983;3:203-210.
11. BENSON RC, FARROW GM, KINSEY JH, et al. Detection and localization of in situ carcinoma of the bladder with hematoporphyrin derivative. Mayo Clin Proc 1982;57:548-555.
12. BRUCE BA. Evaluation of hematoporphyrin photoradiation therapy to treat choroidal melanoma. Lasers Surg Med 1984;4:59-64.
13. DOUGHERTY TJ, LAWRENCE G, KAUFMAN GH, et al. Photoradiation in the treatment of recurrent breast carcinoma. J Natl Cancer Inst 1979;62:231-236.
14. WILE AG, DAHLMAN A, BURNS RG, et al. Laser photoradiation therapy of cancer following hematoporphyrin sensitization. Lasers Surg Med 1982;2:163-168.
15. NELSON JS, LIAW L-H, BERNS MW. Mechanism of tumor destruction in photodynamic therapy. Photochem Photobiol 1987;46:829-836.
16. NELSON JS, WRIGHT WH, BERNS MW. Histopathological comparison of the effects of hematoporphyrin derivative on two different murine tumors using computer enhanced digital video fluorescence microscopy. Cancer Res 1985;45:5781-5786.
17. ROBERTS WG, SHIAU F-Y, NELSON JS, et al. In vitro characterization of monoaspartyl chlorin e_6 and diaspartyl chlorin e_6 for photodynamic therapy. J Natl Cancer Inst 1988;80:330-336.
18. NELSON JS, ROBERTS WG, BERNS MW. In vivo studies on the utilization of mono-L-aspartyl chlorin (NPe6) for photodynamic therapy. Cancer Res 1987;47:4681-4685.
19. SELMAN SH, KREIMER-BIRNBAUM M, KLAUNIG JE, et al. Blood flow in transplantable bladder tumors treated with hematoporphyrin derivative. Cancer Res 1984;44:1924-1927.
20. STAR WM, MARIJNISSEN HPA, VAN DEN BERG-BLOK AE, et al. Destruction of rat mammary tumor and normal tissue microcirculation by hematoporphyrin derivative photoradiation observed in vivo in sandwich observation chambers. Cancer Res 1986;46:2532-2540.
21. HENDERSON BW, WALDOW SM, MANG TS, et al. Tumor destruction and kinetics by tumor cell death in two experimental mouse tumors following photodynamic therapy. Cancer Res 1985;45:572-576.
22. JAIN RK. Transport of macromolecules in tumor microcirculation. Biotechnol Res 1985;1:81-84.
23. JAIN RK. Transport of molecules in the tumor interstitium: a review. Cancer Res 1987;47:3039-3051.
24. COMPER WD, LAURENT TC. Physiological function of connective tissue polysaccharides. Physiol Rev 1978;58:255-315.
25. LAURENT TC. Structure, function and turnover of the extracellular matrix. Adv Microcirc 1987;13:15-34.
26. GULLINO PM, GRANTHAM FH. The influence of the host and the neoplastic cell population on the collagen content of a tumor mass. Cancer Res 1963;23:648-653.
27. MUSSER DA, WAGNER JM, DATTA-GUPTA N. The interaction of tumor localizing porphyrins with collagen and elastin. Res Commun Chem Pathol Pharmacol 1982;36:251-259.

Efficacy of Antibodies to Epidermal Growth Factor Receptor Against KB Carcinoma In Vitro and in Nude Mice

*Esther Aboud-Pirak, Esther Hurwitz, Michael E. Pirak, Francoise Bellot, Joseph Schlessinger, Michael Sela**

Iodine-125-labeled monoclonal antibody 108.4 (108.4 mAb), raised against the extracellular domain of the epidermal growth factor (EGF) receptor, was shown to visualize sc xenografts of human oral epidermoid carcinoma (KB) cells in nude mice. In vitro, although EGF caused an increase in the number of KB cell colonies (150% at a concentration of 160 m*M*), the anti-EGF receptor antibodies reduced clone formation. At a concentration at which EGF caused a 50% increase in colony number, the addition of a 100-fold molar excess of 108.4 mAb resulted in a decrease in the number of cell colonies to 20% of the original value. Therefore, the effect of the antibody on the KB tumor was studied in vivo in three different modes of tumor transplantation. Antitumor activity was demonstrated first by retardation (versus controls) of the growth of tumor cells as sc xenografts ($P > .017$), then by prolongation of the life span of animals with the ip form of the tumor ($P < .001$), and finally on an experimental lung metastasis by a reduction in the number and size of tumors ($P < .05$). When the anti-EGF receptor antibodies were added together with cisplatin, the antitumor

Received July 21, 1988; revised September 26, 1988; accepted September 27, 1988.

Supported in part by "Keren Yeda," The Weizmann Institute of Science.

E. Aboud-Pirak, E. Hurwitz, and J. Schlessinger, Department of Chemical Immunology, The Weizmann Institute of Science, Rehovot, Israel.

M. Pirak, Life Science Research Israel Ltd., Ness Ziona, Israel.

F. Bellot and J. Schlessinger, Rorer Biotechnology, Inc., King of Prussia, PA.

We thank Dr. E. Livneh for helpful advice and suggestions and Mrs. B. Sheiba for typing the manuscript.

**Correspondence to:* Dr. Michael Sela, Department of Chemical Immunology, The Weizmann Institute of Science, Rehovot 76100, Israel.